Poly(ethylene oxide)–*p*-Dihalogenobenzene Crystalline Complex: FTIR and X-ray Diffraction Study of Spherulitic Fibers

J. J. Point and P. Damman*

Université de Mons Hainaut, Laboratoire de Chimie Physique-Thermodynamique, Place du Parc, 20, B-7000 Mons, Belgium

Received January 3, 1990; Revised Manuscript Received September 26, 1990

ABSTRACT: FTIR spectroscopy and X-ray diffraction were used to confirm the crystalline structure of the intercalates formed with poly(ethylene oxide) as the host compound and *p*-dihalogenobenzene as the guest compound. The distinction between the two possible unit cells for the complex was made from the values of the dichroic ratio of the IR absorption bands and from the X-ray diffraction patterns of spherulitic fibers. This paper also gives a first insight into the problem of conformation of the individual macromolecules in these intercalates.

Introduction

Poly(ethylene oxide) (PEO) forms crystalline complexes with small molecules such as urea, thiourea, mercuric halides, resorcinol, etc.,[1-5] in which strong interactions between PEO and the host molecules occur. This paper does not deal with such complexes but with the structures formed by PEO and *p*-dihalogenobenzenes. In these complexes, only weak intermolecular forces are involved and they are formed because the external surface of the PEO macromolecule, in its state of minimum intramolecular energy, presents valleys, the size and shape of which are such that they accommodate specific small molecules such as *p*-dihalogenobenzenes. An exact model in which PEO sheets alternate with benzenic layers was previously proposed for the $[(CH_2CH_2O)_{10}(p\text{-}C_6H_4XY)_3]_n$ intercalates (X and Y being F, Cl, Br, or I)[6-9] (Figure 1). The aim of the present paper is to give additional support for the proposed structure, which is also discussed in another paper on the basis of neutron scattering data. The primitive subcell of the *Cmc*21 orthorhombic cell is, *fortuitously* from our point of view, pseudohexagonal (Figure 1). To rule out definitively a hypothetical true hexagonal structure, we study spherulitic fibers. In such samples, the direction of fastest growth (fiber axis) would be normal to the chain axis. Therefore, X-ray diffraction patterns and IR spectra allow a clear distinction between the hexagonal and orthorhombic symmetries. This paper also deals with a more general problem: we have studied the orientation of the PEO sheets (i.e., (100) plane) with respect to the crystalline growth front. At a sufficiently low rate of crystallization, it may be assumed that in these sheets each macromolecule is adjacently folded (according to Keller's model[10]) in a molecular ribbon, the plane of which is normal to the radius of the spherulite. However, other crystallization models are also plausible. The discussion of this question on experimental grounds gives a first insight into the problem of the conformation of individual macromolecules in these intercalates.

Background Method

a. Crystalline Structure of Intercalates. In polymers, a pseudohexagonal primitive subcell is very often observed because macromolecules are, roughly speaking, nearly cylindrical. In intercalates, where PEO and *p*-dihalogenobenzene layers respectively alternate, there is no reason for a definite relation between the values of *a* and *b* parameters of an orthorhombic subcell. From Table I, we can note that the square of the ratio of parameters *a* and *b* of the *Cmc*21 unit cell proposed for the intercalates

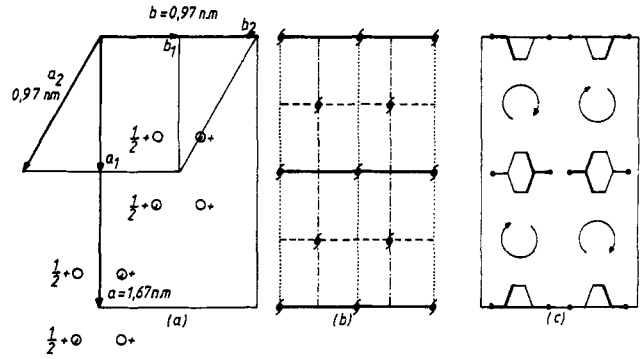

Figure 1. (a) Primitive monoclinic unit cell and *Cmc*21 orthorhombic unit cell, (b) symmetry elements, (c) disposition of the PEO and $p\text{-}C_6H_4XY$ molecules.

Table I
Unit Cells and $(a/b)^2$ Ratios of Intercalates

guest molecules	*a*, nm	*b*, nm	*c*, nm	$(a/b)^2$
$p\text{-}C_6H_4Cl_2$	1.648	0.951	2.786	3.003
$p\text{-}C_6H_4Br_2$	1.674	0.968	2.798	2.991
$p\text{-}C_6H_4ClBr$	1.658	0.958	2.810	2.995
$p\text{-}C_6H_4BrF$	1.638	0.946	2.856	2.998
$p\text{-}C_6H_4ClI$	1.678	0.973	2.824	2.974

equals 3, at the precision of the measurement, whatever is the nature of the guest molecules (despite an appreciable difference between the van der Waals radii of the different halogen atoms). Therefore, the validity of the orthorhombic subcell is open to question. The choice between the *Cmc*21 orthorhombic subcell and a hypothetical true hexagonal cell (with $a = b = 0.951$ nm and $c = 2.786$ nm for $[(CH_2CH_2O)_{10}(p\text{-}C_6H_4Cl_2)_3]_n$)[8] is not possible either on examination of the X-ray fiber diagrams or on the basis of the dichroic ratios of the IR absorption bands of drawn samples. To rule out the possibility of a true hexagonal arrangement of host and guest molecules, we must study samples showing another orientation texture. In the model of Point and Coutelier,[6] PEO and *p*-dihalogenobenzene sheets are alternatively stacked normal to the *a* axis. The X-ray and polarized IR studies of fibers with either an *a* axis or a *b* axis must allow us to confirm or invalidate the orthorhombic model. It was previously pointed out that spherulitic crystallization is a way to prepare such a fiber.[11] In a diametral section of a spherulite, the chain axis (*c* crystallographic direction) is perpendicular to the radius of the spherulite and a definite crystallographic plane is presumed to be parallel to the growth front.

b. Molecular Conformation of the PEO Macromolecules. Because the PEO molecules in the intercalate

0024-9297/91/2224-2019$02.50/0

Table II
Observed and Calculated Components of Reciprocal Vectors from the X-ray Fiber Diagram of Zonal Solidification of $[(CH_2CH_2O)_{10}(p\text{-}C_6H_4Br_2)_3]_n$[a]

θ	hkl	S_y^{obs}, nm^{-1}	S_z^{obs}, nm^{-1}	S_y^{cal}, nm^{-1}	S_z^{cal}, nm^{-1}
10.1	023	2.230	0.0	2.290	0.0
12.9	026	2.824	0.0	2.898	0.0
18.7	043	3.942	0.0	4.031	0.0
5.1	200	0.0	1.160	0.0	1.194
10.3	206	1.904	1.103	2.093	1.194
	220	1.904	1.103	2.018	1.194
11.3	223	2.106	0.918	2.267	1.194
13.9	226	2.708	1.177	2.870	1.194
9.1	303	0.903	1.716	1.018	1.792
10.1	313	1.249	1.731	1.428	1.792
10.6	400	0.0	2.357	0.0	2.389
13.9	406	1.766	2.354	1.991	2.389
14.6	420	1.908	2.323	1.917	2.389
16.8	416	2.534	2.375	2.212	2.389
14.7	513	0.841	2.899	1.216	2.986

[a] Fiber axis a; S_z and S_y are the axial and radial components of the **S** vector.

Table III
Observed and Calculated Components of the Reciprocal Vectors from the X-ray Diffraction Fiber Diagram of a Peripheral Part of a Spherulite of $[(CH_2CH_2O)_{10}(p\text{-}C_6H_4Cl_2)_3]_n$[a]

θ	hkl	S_y^{obs}, nm^{-1}	S_z^{obs}, nm^{-1}	S_y^{cal}, nm^{-1}	S_z^{cal}, nm^{-1}
9.6	006	2.122	0.0	2.123	0.0
10.9	400	2.401	0.0	2.384	0.0
	206	2.401	0.0	2.426	0.0
15.6	209	3.356	0.0	3.326	0.0
16.4	600	3.523	0.0	3.494	0.0
19.1	606	4.017	0.0	3.998	0.0
7.2	013	1.105	1.188	1.062	1.051
10.4	313	1.998	1.199	2.070	1.051
15.2	513	3.138	1.138	3.095	1.051
9.3	020	0.0	1.992	0.0	2.103
10.8	220	1.060	2.188	1.125	2.103
11.8	223	1.404	2.221	1.528	2.103
13.4	323	1.940	2.131	2.086	2.103
	026	1.940	2.131	2.037	2.103
14.4	226	2.312	2.249	2.334	2.103
19.0	620	3.372	1.967	3.376	2.103
19.6	623	3.484	1.991	3.508	2.103
17.4	333	1.758	3.283	1.799	3.154

[a] Fiber axis b; S_z and S_y are the axial and radial components of the **S** vector.

Table IV
Fiber Axis Observed for the $[(CH_2CH_2O)_{10}(p\text{-}C_6H_4XY_4)_3]_n$ Intercalate

sample	M_w	guest molecules	fiber axis
spherulite	2×10^3	p-$C_6H_4Br_2$	a
	6×10^3	p-$C_6H_4Br_2$	a
	2×10^4	p-$C_6H_4Br_2$	a
	2×10^5	p-$C_6H_4Br_2$	b
	2×10^3	p-$C_6H_4Cl_2$	b
	6×10^3	p-$C_6H_4Cl_2$	b
	2×10^5	p-$C_6H_4Cl_2$	b
	2×10^5	p-$C_6H_4Cl_2$	b
zonal solidification	6×10^3	p-$C_6H_4Br_2$	a
	6×10^3	p-$C_6H_4Cl_2$	a
	6×10^3	p-C_6H_4ClBr	a
	6×10^3	p-C_6H_4ClI	a

adopt a 10/3 helical conformation very similar to the 7/2 helix observed in pure PEO, and because in a PEO sheet the distance between the nearest oppositely handed chains is nearly equal to that observed in the pure polymer,[12] it was proposed that PEO sheets are made of macromolecules adjacently folded in a Keller molecular ribbon[10] parallel to the (100) crystallographic plane. In the framework of the generally accepted theories of polymer crystallization, it may also be assumed that such molecular sheets are parallel to the growth front and thus normal to the spherulitic radius. If such an orientation were observed, this would reinforce a unified picture of idealized structures of polymer single crystals.

Experimental Section

Two types of PEO samples were used, an oligomer with M_w 6000 and M_w/M_n 1.1 (Hoechst) and a polymer with M_w 200 000 (Aldrich). Spherulitic fibers were prepared by melting or by zonal solidification as proposed by Lovinger.[13] X-ray diffraction diagrams were taken with Cu Kα radiation. IR spectra were obtained on a Bruker IFS113V Fourier transform infrared spectrometer. Thirty-two co-added interferograms were scanned with a resolution of 2 cm^{-1}. An aluminum wire grid polarizer from SPECAC was used for recording polarized spectra. Dichroic ratios are defined by the following relation: $R = A_\parallel/A_\perp$ where $A_\parallel$ and $A_\perp$ are the peak optical densities with electric vector parallel or perpendicular to the fiber axis.

To discuss the polarization of p-dihalogenobenzene vibrations, we made use of a trirectangular system OX, OY, OZ. The OX and OZ axes were respectively the normal to the benzenic plane and the 1–4 axis. The assignments proposed by Varsanyi for benzenic vibrations[14] were used in this work. To characterize the dispersion of the orientation of the crystals in a sample, we used the second-order moment of the orientation function defined by the relation

$$P_2(\theta) = \frac{(R-1)(R_0-2)}{(R+2)(R_0-1)}$$

where R is the experimental dichroic ratio and R_0 is the dichroic ratio for a perfectly oriented fiber, calculated by the relation

$$R_0 = 2 \cot g^2 \alpha$$

α being the angle between the fiber axis and the dipole moment vector of the vibration.

Results

a. X-ray Diffraction Data. Figure 2 shows the X-ray fiber diagrams of the $[(CH_2CH_2O)_{10}(p\text{-}C_6H_4Br_2)_3]_n$ intercalate prepared by zonal solidification and of a peripheral part of a spherulite of $[(CH_2CH_2O)_{10}(p\text{-}C_6H_4Cl_2)_3]_n$ (PEO M_w 6000), the axes of which are respectively a and b. Tables II and III indicate the comparison of observed and calculated positions (on the basis of the orthorhombic cell) of the diffraction spots for these two samples. The orientation of the fiber axes observed for the variously studied samples is given in Table IV. Note that, for the same intercalate (PEO M_w 6000, p-$C_6H_4Cl_2$ for instance), we observed different fiber axes. As noted by a reviewer, this is a puzzling feature because the zone-solidified material consists of spherulithic fibers. But in fact, as observed in pure oligomeric PEO[15] and in the present system, the orientation of the crystals depends on the temperature of crystallization. In the spherulite crystallizations, this temperature is held at 25 °C. In the zone solidification experiments, the crystallization temperature is higher and unknown. In oligomeric PEO, even when folded, the molecule is not a wide molecular ribbon, and this diversity of orientation of the crystals with respect to the fiber axis does not represent a major problem. The orientation of the polymeric samples with respect to the fiber axis is described later in the Mechanism of Crystallization and Conformation of the PEO Macromolecules subsection.

b. IR Spectroscopy. Polarized IR spectra of spherulitic fibers of the $[(CH_2CH_2O)_{10}(p\text{-}C_6H_4Br_2)_3]_n$ intercalate prepared by zonal solidification are shown in Figure 3. The assignments and dichroic ratios for PEO and ben-

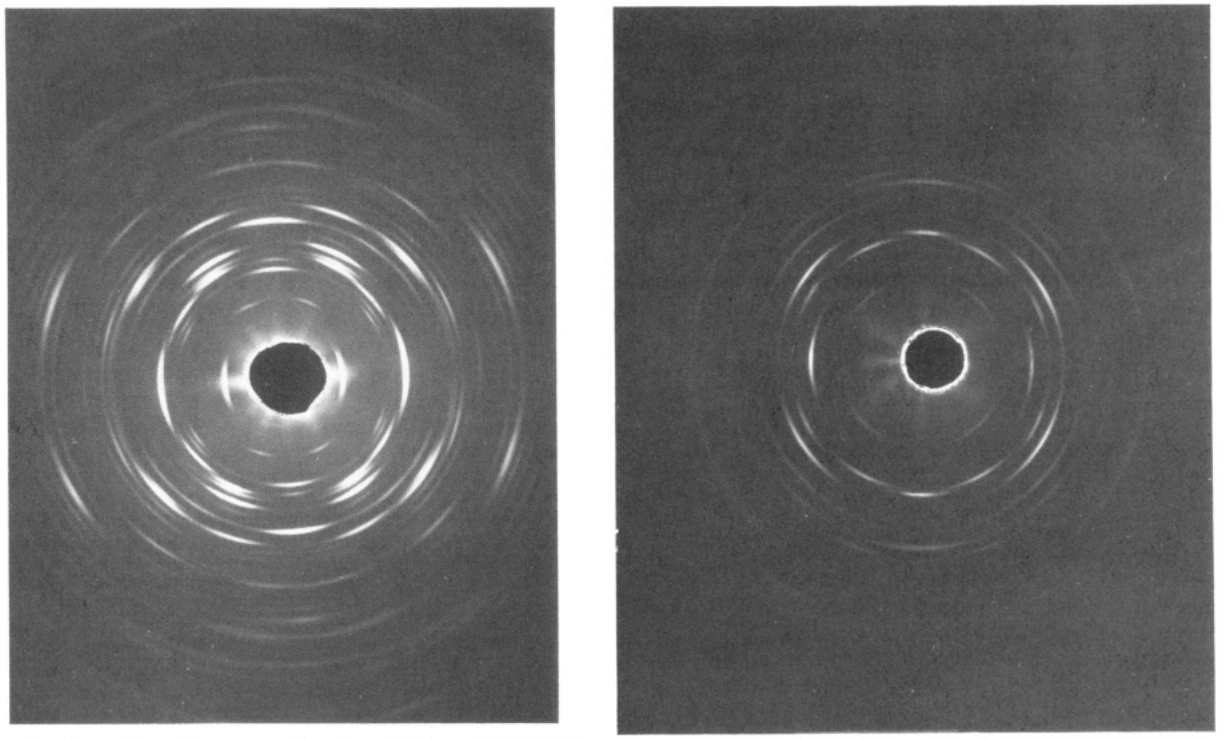

Figure 2. X-ray fiber diagrams of various PEO–p-C_6H_4XY intercalates: (left) XY, BrBr (fiber axis a); (right) XY, ClCl (fiber axis b).

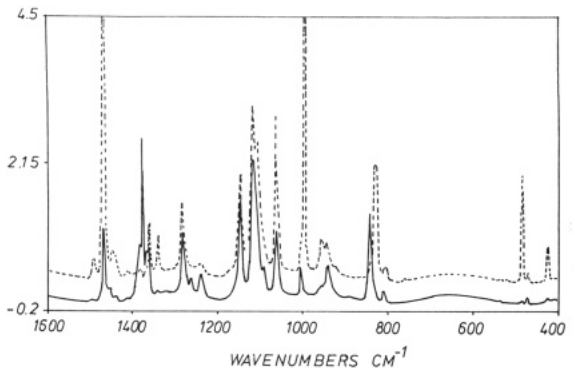

Figure 3. Polarized IR spectra of PEO–p-$C_6H_4Br_2$ spherulitic fibers. The solid (or broken) line represents the spectrum measured with the electric vector parallel (or perpendicular) to the fiber axis.

zenic vibrations in all the samples are given in Tables V and VI. The values of α and $P_2(\Theta)$ are also given by assuming that the unit cell is orthorhombic.

c. Splitting of the E1 Vibrations of PEO. We have observed in all samples the splitting of E1 vibrations of the PEO in two components, one corresponding to the electric vector parallel, the other corresponding to the electric vector perpendicular to the fiber axis that is not parallel to the c crystallographic direction (Figure 4). The values of the wavenumbers for the two components are listed in Table VII for all the samples. We thus obtain a *very direct proof* of the validity of an orthorhombic unit cell for the intercalates. Accordingly, we have confirmed previously given results.[7,9] The A2 doublet at 529–509 cm^{-1} in pure PEO is shifted to 523–515 cm^{-1} in the intercalates. The wavenumbers of the out-of-plane vibrations 16b and 17b are shifted to higher frequencies. These modifications result from the interactions between host and guest molecules.

Discussion

a. Crystalline Structure of the Intercalates. The possibility of a true hexagonal structure for the intercalates is definitively ruled out by this present experimental work. Three proofs supporting this conclusion are given in this paper.

(i) In the two types of X-ray fiber diagrams (a or b), the positions of the diffraction spots do not obey hexagonal symmetry.

(ii) We know, from a study of drawn samples,[7] that the OY axis of the disubstituted benzenic molecule is normal to the chain axis and that the 1–4 OZ axis makes an angle of 35°. In the study of spherulitic fibers, the chain axis is perpendicular to the fiber axis (a or b). Then, in such fibers, the dichroic ratios, predicted from any hexagonal model for benzenic vibrations polarized according to the

Table V
Assignments, Dichroic Ratios, α, and $P_2(\Theta)$ for Benzenic Vibrations

sample	mode	freq, cm^{-1}	axis	R	α, deg	$P_2(\Theta)$
		Spherulite				
p-$C_6H_4Br_2$	20a	426	OZ	0.08	90	0.885
PEO M_w 6×10^3	16b	486	OX	0.04	90	0.941
fiber axis a	20b	3084	OY	15.4	0	0.828
p-$C_6H_4Cl_2$	16b	499	OX	2.13	35	0.597
PEO M_w 2×10^5	20a	543	OZ	1.7	55	
fiber axis b	19b	1394	OY	0.23	90	0.691
	20b	3085	OY	0.23	90	0.691
		Zonal Solidification				
p-$C_6H_4Br_2$	20a	429	OZ	0.1	90	0.857
PEO M_w 6×10^3	16b	486	OX	0.02	90	0.970
fiber axis a	18a	999	OZ	0.03	90	0.956
	20b	3082	OY	28.0	0	0.900
p-$C_6H_4Cl_2$	16b	499	OX	0.21	90	0.715
PEO M_w 6×10^3	20a	543	OZ	0.25	90	0.667
fiber axis a	19b	138	OY	5.5	0	0.600
	20b	309	OY	5.3	0	0.589
p-C_6H_4ClBr	16b	496	OX	0.21	90	0.715
PEO M_w 6×10^3	19b	1389	OY	10.8	0	0.766
fiber axis a	20b	3086	OY	6.8	0	0.659
p-C_6H_4ClI	16b	489	OX	0.05	90	0.927
PEO M_w 6×10^3	18a	1000	OZ	0.02	90	0.979
fiber axis a	20a	3078	OY	75.0	0	0.961

Table VI
Assignments, Dichroic Ratios, α, and $P_2(\Theta)$ for PEO Vibrations

sample	mode	freq, cm^{-1}	R	α, deg	$P_2(\Theta)$
		Spherulite			
	E1	844	1[a]		
p-$C_6H_4Br_2$	E1	945	1[a]		
	A2	958	0.38[b]	0	0.521
PEO M_w 6×10^3	E1	1284	1[a]		
	A2	1342	0.38	0	0.521
fiber axis a	E1, A2	1466	0.50		
p-$C_6H_4Cl_2$	A2	529	1.23		
	E1	943	1.03		
PEO M_w 2×10^5	A2	956	1.12[b]		
	E1	1282	1.00		
fiber axis b	A2	1342	1.10		
	A2	1453	1.67		
	E1	1469	b		
		Zonal Solidification			
p-$C_6H_4Br_2$	E1	947	1[a]		
	A2	958	0.25[b]	0	0.667
PEO M_2 6×10^3	E1	1147	1[a]		
	E1	1278	1[a]		
fiber axis a	A2	1342	0.10	0	0.857
	E1, A2	1469	0.26		
p-$C_6H_4Cl_2$	A2	526	0.10	0	0.857
	E1	944	1[a]	0	
PEO M_w 6×10^3	A2	954	0.61[b]	0	0.299
	E1	1060	1[a]		
fiber axis a	E1	1282	1[a]		
	A2	1342	0.56	0	0.344
	A2	1453	0.5[b]	0	0.400
	E1	1469	1[a]		
p-C_6H_4ClBr	A2	525	0.06	0	0.912
	E1	944	1[a]		
PEO M_w 6×10^3	A2	955	0.3[b]	0	0.609
	E1	1060	1[a]		
fiber axis a	E1	1147	1[a]		
	E1	1282	1[a]		
	A2	1342	0.14	0	0.804
	A2	1455	0.32[b]	0	0.586
	E1	1469	1[a]		
p-C_6H_4ClI	A2	523	0.00	0	1.00
	E1	945	1[a]		
PEO M_w 6×10^3	A2	958	0.19[b]	0	0.740
	E1	1060	1[a]		
fiber axis a	E1	1282	1[a]		
	A2	1344	0.07	0	0.893
	E1	1464	1[a]		

[a] Vibration splitting in two components. [b] Superposition of several vibrations.

OX or OZ axis, would be significantly different from zero because in any hexagonal model the 6-fold axis must be parallel to the axis of the PEO chain. However, experimental dichroic ratios for these vibrations are nearly zero when the fiber axis is a.

(iii) No splitting of the E1 vibrations of the PEO can be observed if the unit cell is hexagonal.

In addition, the experimental results are in good agreement with the orthorhombic unit cell.

(i) The orthorhombic unit cell can explain the exact positions of the diffraction spots in the three types of fibers, c fibers (previously described) and a and b fibers (this work, Tables II and III).

(ii) The orthorhombic model gives results in accordance with the observed dichroic ratios. The values of the second-order moment of the orientation function ($P_2(\Theta)$) were calculated by assuming cylindrical symmetry around the fiber axis (clearly an oversimplification). The results of this calculation is given in Tables V and VI. The general but not perfect agreement between calculated and observed values gives confidence in the proposed molecular model

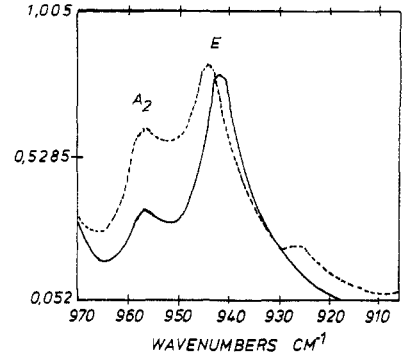

Figure 4. Polarized IR spectra of PEO–p-$C_6H_4Br_2$ spherulitic fibers. The solid (or broken) line represents the spectrum measured with the electric vector parallel (or perpendicular) to the fiber axis.

Table VII
Values of the Wavenumbers and the Frequency Shift for E1 Vibrations of PEO in Various Intercalates

	wavenumber, cm^{-1}		
sample	pure polymer	components in intercalate	shift (perp–par)
	Spherulite		
p-$C_6H_4Br_2$	947	944.1	1.9
		942.2	
PEO M_w 6×10^3	1278	1282.6	2.9
		1279.7	
fiber axis a			
p-$C_6H_4Cl_2$	947	943.1	−1.0
		944.1	
PEO M_w 2×10^5	1278	1281.7	−0.9
		1282.6	
fiber axis b			
	Zonal Solidification		
p-$C_6H_4Br_2$	947	944.1	1.9
		942.2	
PEO M_w 6×10^3	1278	1282.6	2.9
		1279.7	
fiber axis a			
p-$C_6H_4Cl_2$	947	945.1	2.0
		943.1	
PEO M_w 6×10^3	1278	1282.6	0.9
		1281.7	
fiber axis a			
p-C_6H_4ClBr	947	945.1	2.9
		942.2	
PEO M_w 6×10^3	1278	1282.6	1.9
		1280.7	
fiber axis a			

for the intercalates. For a more detailed discussion and more precise predictions, the real dispersion of the orientation of the crystals in a sample must be known. In the case of a spherulitic fiber, the crystallographic parameter (a or b) can depart from the fiber axis for two reasons. Firstly, departure is relative to the experiments themselves: the irradiated part of the spherulite in FTIR measurements is of a finite extent. This leads to a dispersion of fiber axes in the plane of the samples. Secondly, there is a dispersion of the fiber axes out of the plane of the samples, resulting from the three-dimensional growth of a spherulite (for a more complete description of the spherulitic growth, see Keith[16] or Basset et al.[17] for instance). Some work is being undertaken to elucidate this rather specialized question, but we limit ourselves in the present paper to note that the values of the observed dichroic ratios confirm qualitatively the previously described orthorhombic model.

b. Mechanism of Crystallization and Conformation of the PEO Macromolecules. The orientation of the

unit cell with respect to the growth front depends on the molecular weight of the PEO used to prepare the intercalates.

(i) For samples made from low molecular weight PEO, the direction of fastest growth depends on the p-dihalogenobenzene molecules used and the conditions of crystallization. This growth direction is either *a* or *b*. This problem requires a more complete investigation. However, such results are not completely unexpected. Indeed, Balta Calleja et al.[15] have observed in pure PEO that various crystallographic planes may be normal to the spherulitic radius, and we have confirmed this result (in preparation).

(ii) A completely unexpected result is obtained for both samples in which the host molecule is a high molecular weight polymer. The *b* axis of the crystal is parallel to the spherulitic radius. However, Point and Coutelier[6] have assumed that each macromolecule is adjacently folded in a Keller molecular ribbon[10] and confined to a (100) plane, and the theories of polymer crystallization predict that a macromolecule is adjacently folded in a plane parallel to the growth front of crystallization. However, the growth front is in fact *not parallel* to the (100) plane. Moreover, this assumed conformation of the PEO molecules has not been proved. It may be that each macromolecule is confined to an (010) plane and regularly folded in the *second* adjacent position, the first being occupied by the p-dihalogenobenzene molecules. In the case of pure polymer samples, suggestions in this direction were previously made by Flory and Yoon.[18] It may also be that the macromolecules reenter in the crystal in a more or less random way. We have not enough data to make a choice between these various possibilities. This question justifies the study by small-angle neutron scattering of intercalates made from a mixture of hydrogenated and deuterated PEO. In the intercalate, the distance between PEO sheets being increased (with respect to the one observed in pure PEO) by the presence of p-dihalogenobenzene molecules, the three considered conformations (an adjacent folding, a reentry in the second adjacent position, and a random reentry) must lead to *very* different SANS diagrams. The preparation of oriented samples by zonal solidification opens interesting possibilities in such a study.

Conclusions

(i) Crystalline Structure of the Intercalate. Three experimental facts discard definitively a possible true hexagonal subcell and confirm the validity of the *Cmc*21 orthorhombic unit cell for the intercalate. Firstly, the positions of the diffraction spots for the *a* or *b* X-ray fiber diagrams do not show a hexagonal symmetry and are explained exactly by the orthorhombic cell. Secondly, the dichroic ratios measured by FTIR are in agreement with the orthorhombic crystalline model. Lastly, the splitting of the E1 vibrations of PEO gives direct proof of the validity of the orthorhombic unit cell.

(ii) Conformation of the PEO Molecule. We have observed, for the samples prepared with high molecular weight PEO, that the *b* axis of the crystal is parallel to the spherulitic radius. To explain these observations, we can propose three different conformations for the PEO macromolecules: (i) an adjacent folding in a (100) plane, (ii) a folding in the second adjacent position in an (010) plane, or (iii) a random reentry. In this first case, each individual molecule is confined to a plane *normal* to the growth front. For pure polymers, suggestions in this direction have been made by Sadler.[19] But both this possibility and the random reentry are in total contradiction with the usually accepted theories of crystallization. This point is to be scrutinized by SANS study.

Acknowledgment. We are indebted to Mr. Lefebvre for the X-ray experiments. This work was supported by the Ministère de la Région Wallonne (programme de formation et d'impulsion à la recherche scientifique et technologique) and by the F.N.R.S. (Fond National de la Recherche Scientifique, Belgium).

References and Notes

(1) Tadokoro, H.; Yoshihara, T.; Chatani, Y.; Nakanishi, F. *J. Polym. Sci. B* **1964**, *2*, 363.
(2) Iwamato, R.; Saito, Y.; Ishihara, H.; Tadokoro, H. *J. Polym. Sci. A2* **1968**, *6*, 1509.
(3) Myasnikova, R. M.; Titova, E. F.; Obolonkova, E. S. *Polymer* **1980**, *21*, 403.
(4) Point, J. J.; Delaite, E.; Dosière, M. Submitted to *Macromolecules*.
(5) Point, J. J.; Delaite, E.; Dosière, M. To be published.
(6) Point, J. J.; Coutelier, C. *J. Polym. Sci., Polym. Phys. Ed.* **1985**, *22*, 231.
(7) Point, J. J.; Jasse, B.; Dosiere, M. *J. Phys. Chem.* **1986**, *90*, 3273.
(8) Point, J. J.; Coutelier, C.; Villers, D. *J. Phys. Chem.* **1986**, *90*, 3277.
(9) Point, J. J. *J. Inclusion Phenom.* **1988**, *6*, 253.
(10) Keller, A. *Faraday Discuss. Chem. Soc.* **1979**, *68*, 145.
(11) Point, J. J. *Bull. Cl. Sci., Acad. R. Belg.* **1953**, *39*, 453.
(12) Takahashi, Y.; Tadokoro, H. *Macromolecules* **1973**, *6*, 672.
(13) Lovinger, A. J.; Gryte, C. C. *Macromolecules* **1976**, *2*, 247.
(14) Varsanyi, G. *Vibrational spectra of benzene derivatives*; Academic Press: New York, 1969.
(15) Balta, Calleja, F. J.; Hay, I. L.; Keller, A. *Kolloid Z. Z. Polym.* **1966**, *209*, 128.
(16) Keith, H. D. *J. Polym. Sci. A* **1964**, *2*, 4339.
(17) Basset, D. C.; Olley, R. H. *Polymer* **1984**, *25*, 935.
(18) Flory, P. J.; Yoon, D. Y. *Faraday Discuss. Chem. Soc.* **1979**, *68*, 288.
(19) Sadler, D. M. *Nature* **1987**, *326*, 174.

Registry No. PEO·$pC_6H_4Cl_2$, 88882-54-6; PEO·$pC_6H_4Br_2$, 102073-61-0; PEO·pC_6H_4BrCl, 102073-58-5; PEO·pC_6H_4BrF, 102073-59-6; PEO·pC_6H_4ClI, 102073-60-9.